ChemComm

COMMUNICATION

View Article Online
View Journal | View Issue

Cite this: *Chem. Commun.*, 2016, 52, 7719

Received 15th April 2016,
Accepted 17th May 2016

DOI: 10.1039/c6cc03149h

www.rsc.org/chemcomm

A MOF-derived Co–CoO@N-doped porous carbon for efficient tandem catalysis: dehydrogenation of ammonia borane and hydrogenation of nitro compounds†

Xiao Ma,‡ Yu-Xiao Zhou,‡ Hang Liu, Yang Li and Hai-Long Jiang*

The one-step pyrolysis of a zeolite-type metal–organic framework, Co(2-methylimidazole)$_2$ (ZIF-67), produces an N-doped porous carbon incorporating well-dispersed Co/CoO nanoparticles, which exhibit excellent catalytic activity, chemoselectivity and magnetic recyclability for the tandem dehydrogenation of ammonia borane and hydrogenation of nitro compounds at room temperature.

Aromatic and aliphatic amines are high-value chemicals with wide applications for the manufacture of dyes, pigments, food additives, pharmaceuticals, herbicides and fine chemicals.[1] These amines are generally prepared *via* the hydrogenation of corresponding nitro compounds, while the co-existence of other reducible functional groups in them poses challenges for selective reduction.[1] Currently, selective hydrogenation of nitroarenes mostly relies on noble metal-based catalysts which have a high price and scarcity limitations.[2] Therefore, heterogeneous catalysts based on earth-abundant base metals (for example, Fe, Co and Ni) are highly desired.[3] For this purpose, having base metal nanoparticles (NPs) with small sizes stabilized inside a stable porous matrix would be an ideal strategy. In this context, as a relatively new class of porous materials, metal–organic frameworks (MOFs),[4] usually constructed from base metal (clusters) and organic ligands with diversified and tailorable structures, have been primarily demonstrated to be suitable templates/precursors to afford uniform metal (oxide) NPs distributed throughout porous carbon *via* pyrolysis, in which high porosity and long-range structural ordering could be partially preserved.[5] These MOF-derived porous composites have been recently reported in various heterogeneous reactions.[6]

Hefei National Laboratory for Physical Sciences at the Microscale, CAS Key Laboratory of Soft Matter Chemistry, Collaborative Innovation Center of Suzhou Nano Science and Technology, Department of Chemistry, University of Science and Technology of China, Hefei, Anhui 230026, P. R. China. E-mail: jianglab@ustc.edu.cn

† Electronic supplementary information (ESI) available: Detailed experimental procedures and supporting figures. See DOI: 10.1039/c6cc03149h

‡ These authors contributed equally to this work.

On the other hand, the hydrogenation of nitro compounds usually requires hydrogen as the reducing agent at high pressures and/or high temperatures, due to the very low solubility of hydrogen in different solvents. Sufficient contact between the hydrogen gas and nitro compounds would be a prerequisite to boost the reaction efficiency. To meet this challenge, *in situ* hydrogen production coupled with the reduction of nitro compounds would be a suitable solution, as the *in situ*-generated H_2 throughout the reaction system will readily and immediately react with the nitro group, enhancing the reaction efficiency. In this regard, ammonia borane (NH_3BH_3), having a high hydrogen content of 19.6 wt% and a high solubility in water and methanol, is an excellent hydrogen source.[7,8] The coupling of dehydrogenation of NH_3BH_3 and hydrogenation of nitro compounds in a tandem route is expected to greatly boost the reaction rate.[9]

With these things in mind, a zeolite-type MOF, Co(2-methylimidazole)$_2$ (ZIF-67),[10] as a template and precursor, has been pyrolyzed to form a Co–CoO@N-doped porous carbon nanocomposite with a regular shape, where crystalline Co NPs with oxidized CoO species on the surface are evenly distributed throughout the N-doped porous carbon. The resultant nanocomposite exhibits excellent catalytic performance and is magnetically recyclable toward the tandem dehydrogenation of NH_3BH_3 and reduction of nitro compounds at room temperature (Scheme 1). It is worth stressing that the current base metal catalyst takes advantage of *in situ*-generated hydrogen from NH_3BH_3 to efficiently reduce nitrobenzene, for which the catalytic rate/activity (1.5 h, 100%) is several orders of magnitude higher than that using 1 bar H_2 (12 h, 0.7%). In addition, the catalyst is able to selectively convert a variety of substituted aromatic or aliphatic nitro compounds into the corresponding amines with conversions and yields of up to 100% in several hours, tolerating different reducible groups in functionalized nitrobenzene, including nitrile, aldehyde and ketones.

ZIF-67 was easily obtained by stirring $Co(NO_3)_2$ and 2-methylimidazole in water at room temperature.[6b,10] The purity of the ZIF-67 was confirmed using powder X-ray diffraction (PXRD) (Fig. S1a, ESI†). The N_2 sorption results show the typical type I

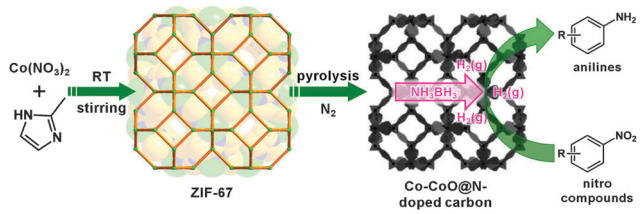

Scheme 1 Schematic illustration of the synthesis of ZIF-67 and its pyrolyzed N-doped porous carbon encapsulating Co–CoO NPs for the tandem catalysis of the dehydrogenation of NH_3BH_3 and hydrogenation of nitro compounds.

isotherm for ZIF-67, matching its microporous character (Fig. S1b, ESI†). The pyrolysis of ZIF-67 nanocrystals at different temperatures under N_2 provides Co–CoO@N-doped porous carbon nanocomposites, denoted as Co-*T*-*t* (*T* and *t* represent pyrolysis temperature and time, respectively; *T* = 500, 600 and 700 °C; *t* = 1, 2 and 3 h). The PXRD patterns for all of the products exhibit three sharp peaks assignable to metallic β-Co at $2\theta = 44.38^\circ$ (111), 51.60° (200) and 75.68° (220) (Fig. S2a, ESI†), confirming the main component, and the peak intensity is dominated by the pyrolysis temperature. The weak C (002) peak at ~25° should be due to the low graphitization degree, supported by the Raman spectra (Fig. S3, ESI†), of the resultant carbons obtained at relatively low pyrolysis temperatures. All of the N_2 sorption isotherms are close to type-IV with a hysteresis loop, and the pore size of Co-500-3 h mainly falls into the range of 1–3 nm with some larger ones from 7 nm (Fig. S4, ESI†). The inductively coupled plasma atomic emission spectrometry (ICP-AES) data present the increased Co content following the elevated pyrolysis temperatures, namely, 21.6%, 29.0%, and 32.7%, respectively for Co-500-3 h, Co-600-3 h, and Co-700-3 h (Table S1, ESI†).

The microstructure observation for ZIF-67 and its pyrolysis product, taking Co-500-3 h as a representative, has been conducted using scanning electron microscopy (SEM) and transmission electron microscopy (TEM). Compared with the original ZIF-67 nanocrystals of 200–500 nm (Fig. 1a), Co-500-3 h exhibits some shrinkage with a relatively uniform size and rough surface (~200 nm, Fig. 1b). The metallic NPs of 6–20 nm in size with high contrast are uniformly distributed in the porous carbon (Fig. 1c and Fig. S5, ESI†). The high-resolution TEM (HRTEM) image affords the evidence of crystalline Co with a lattice spacing of 0.20 nm (Fig. 1d), which is consistent with the powder XRD results (Fig. S2a, ESI†). The SAED pattern exhibits individual rings mainly indexed to the (111), (200), (220) and (311) planes of β-Co, and other rings can be assigned to the planes of CoO (marked with asterisks, Fig. 1d, inset), supporting the surface oxidation of Co to CoO, in agreement with the previous report.[6b] X-ray photoelectron spectroscopy (XPS) analysis verifies the co-existence of Co, C, N and O on the surface of Co-500-3 h (Fig. S6, ESI†), in which the forms of Co include Co(0), Co^{2+} and Co-OH species, as revealed by the Co 2p spectrum (Fig. S7a, ESI†).[11] The Co^{2+} observed is consistent with the above SAED results. In addition, the N 1s spectrum exhibits four distinct peaks (pyridinic, pyrrolic, graphitic and oxidized nitrogen species) with binding energies of 398.6, 399.3, 400.7 and 404.1 eV (Fig. S7b, ESI†). All of the above results suggest that the pyrolysis of ZIF-67 leads to

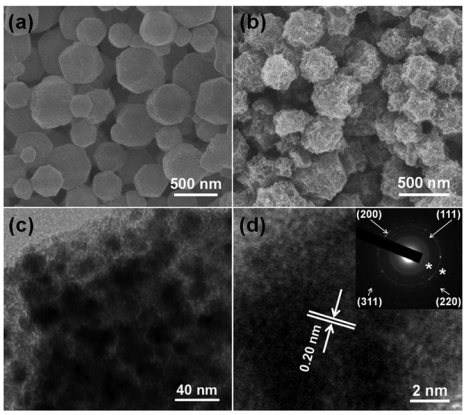

Fig. 1 Microstructure observation for ZIF-67 and Co-500-3 h. SEM images of (a) ZIF-67 and (b) Co-500-3 h. (c) TEM and (d) HRTEM images (inset: SAED pattern) of Co-500-3 h.

crystalline Co NPs, with partially oxidized CoO on the surface, evenly distributed throughout the N-doped porous carbon.

Co NP-based catalysts have been reported to be active in many important processes, including the reduction of nitro compounds,[2,3b] the hydrolysis of NH_3BH_3,[12] *etc.* However, to the best of our knowledge, the tandem dehydrogenation of NH_3BH_3 and hydrogenation of nitro compounds over base metal catalysts remains unreported thus far. The above ZIF-67-derived high-density Co–CoO NPs are uniformly distributed in the porous carbon matrix, in which the pore structure not only facilitates the transportation of substrates/products but also limits the aggregation of the active Co species. These features would make the nanocomposites ideal catalysts for the tandem conversion.

Encouraged by the above considerations, the tandem catalysis using nitrobenzene as a model substrate over ZIF-67-derived nanocomposites was investigated to explore the optimized reaction parameters (Table 1). Due to the great solubility of nitro compounds in methanol but not in water, a methanol/water mixture of 2/3 (v:v) was adopted as an optimized solvent system to form a homogeneous solution of the reactants (Section S2, Fig. S8, ESI†). Among all of the nanocomposites obtained using different pyrolysis temperatures and time lengths, Co-500-3 h showed the best activity and 100% selectivity to complete the reaction and give the target product within 1.5 h (entries 1–8). Unexpectedly, Co/AC offered a very low catalytic activity (entry 9), possibly due to the uneven catalytic sites and low porosity. Strikingly, when NH_3BH_3 was replaced by 1 bar hydrogen while the other conditions remained unaltered, the conversion sharply lowered to 0.7% even after 12 h of reaction (entry 10). It is believed that the *in situ*-generated hydrogen from NH_3BH_3 has a higher solubility/concentration in the reaction solution, which is beneficial to the sufficient contact with nitro compounds, and thus accelerates the reduction of the nitro group. Therefore, the coupling of *in situ* dehydrogenation and hydrogenation reactions should be a very efficient approach. The presence of a Co-based catalyst and NH_3BH_3 as a hydrogen source is necessary for the conversion (entries 11 and 12). The small-size and highly active Co NPs stabilized by the special porous structure of Co-500-3 h play a crucial role in the high catalytic activity and selectivity.

Table 1 Tandem dehydrogenation of NH_3BH_3 and hydrogenation of nitrobenzene over different Co-based nanocomposite catalysts[a]

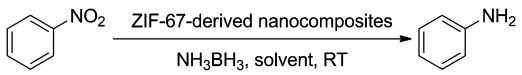

Entry	Catalyst	Time (h)	Yield[b] (%)
1[c]	Co-500-3 h	—	—
2[d]	Co-500-3 h	2	72 (no further conversion)
3	Co-500-3 h	1.5 (1st run)	100
4	Co-500-3 h	1.5 (3rd run)	~100
5	Co-500-1 h	6	44
6	Co-500-2 h	6	37
7	Co-600-3 h	3	100
8	Co-700-3 h	6	100
9	Co/AC	6	3
10[e]	Co-500-3 h	12	0.7
11	—	12	1.4
12[f]	Co-500-3 h	12	~0

[a] Reaction conditions: 0.2 mmol nitrobenzene, 4 mL CH_3OH, 6 mL H_2O, 0.05 mmol catalyst, and 0.6 mmol NH_3BH_3, unless otherwise mentioned. 1 mmol dodecane was added as an internal standard. [b] Determined by GC or GC-MS. [c] Using 10 mL H_2O as a solvent. [d] Using 10 mL CH_3OH as a solvent. [e] NH_3BH_3 was replaced by 1 bar H_2. [f] Without NH_3BH_3.

The stability and recyclability properties of catalysts are of great importance for their practical applications. It can be seen that the activity and selectivity of Co-500-3 h were well retained during three consecutive runs without any treatment or activation of the catalyst (Table 1, entry 4), demonstrating its recyclability. In addition, the Co NPs retain a high level of dispersion and crystallinity and their sizes are almost retained after the catalytic reaction, revealing the good confinement effect of the porous carbon (Fig. 2a and Fig. S9, ESI†). To verify the heterogeneity of the Co-500-3 h catalyst, a filtration test was carried out after 30 min of reaction. No further conversion of nitrobenzene was observed even after 3 h of reaction under identical conditions (Fig. 2b). In addition, the catalyst was easily separated during the reaction using an external magnet due to the strong magnetism of the Co species (Fig. 2b, inset). Therefore, the Co-500-3 h catalyst presents impressive catalytic activity and recyclability, and possesses a truly heterogeneous nature, showing that is has potential application in the chemical industry.

To demonstrate the general applicability of Co-500-3 h in tandem catalysis, a variety of nitro compounds were investigated under the optimized conditions. Different aromatic or aliphatic nitro compounds were converted into the corresponding amines with excellent yields and selectivity (Table 2). The fluoro-, chloro- and bromo-anilines were prepared in excellent yields (100%, entries 1–3). All *ortho*-, *meta*- and *para*-methyl nitrobenzenes were converted rapidly and completely, revealing that slight space steric hindrance to the hydrogenation of the nitro group can be well tolerated (entries 4–6). Moreover, the nitro compounds

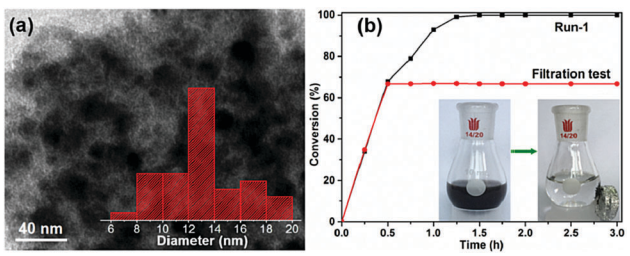

Fig. 2 (a) TEM image of Co-500-3 h (inset: size distribution of the Co NPs) after catalysis. (b) The filtration test for the reduction of nitrobenzene over Co-500-3 h (inset: photographs recording the facile separation of the catalyst *via* an external magnet).

Table 2 Tandem dehydrogenation of NH_3BH_3 and hydrogenation of various nitro compounds over Co-500-3 h[a]

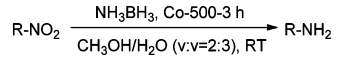

Entry	Substrate	Time (h)	Product	Yield[b] (%)
1	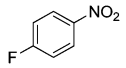	2.5	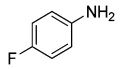	100
2	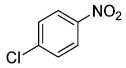	2	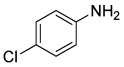	100
3	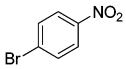	3	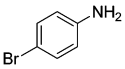	100
4	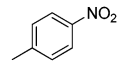	3	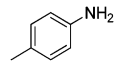	100
5	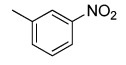	3	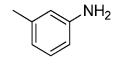	100
6	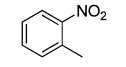	2	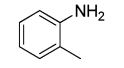	100
7	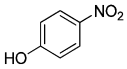	3	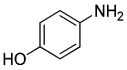	100
8	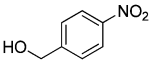	3	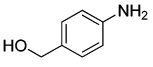	100
9	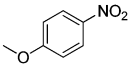	3	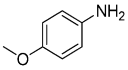	100
10	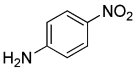	3	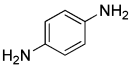	100
11	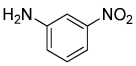	3	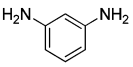	100
12	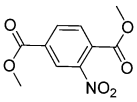	4	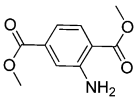	100
13[c]	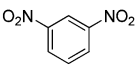	4	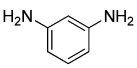	100
14	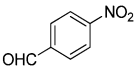	1.5	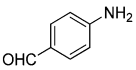	98
15	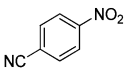	1.5	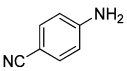	96
16	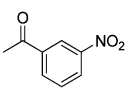	2	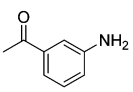	86
17	CH_3NO_2	2	CH_3NH_2	95
18	$CH_3CH_2NO_2$	2	$CH_3CH_2NH_2$	92

[a] Reaction conditions: 0.2 mmol nitro compound, 0.6 mmol NH_3BH_3, 0.05 mmol catalyst, 4 mL of MeOH, and 6 mL of H_2O, at room temperature unless otherwise mentioned. [b] Catalytic reaction products were analyzed and identified by GC and/or GC-MS. [c] 0.1 mmol substrate.

involving electron-rich groups (for example, methyl, *p*-hydroxyl, *p*-methoxy, *p*-methylol and amino, *etc.*) or electron-deficient substituents (such as ester, nitro, aldehyde, ketone and nitrile) were reduced to the corresponding amine products in an efficient fashion with absolute selectively (entries 4–16). Particularly, the nitroarenes functionalized with the most challenging reducible functional moieties, such as aldehyde, ketone and nitrile groups, were successfully reduced to the aniline products with good to excellent selectivity (entries 14–16), highlighting the great chemoselectivity of the Co-based porous nanocatalyst and the remarkable advantage compared to that of noble metal-based catalysts. The –CN and –C═O groups attached to the benzene with electronic/conjugation effects might also partially contribute to the great catalytic selectivity. To our delight, the tandem reaction can be further extended to simple aliphatic nitro compounds, which were converted to the related primary amines with high yields in 2 h (entries 17 and 18). These results again demonstrate that, when coupling with NH_3BH_3 dehydrogenation to afford a hydrogen source, the Co-500-3 h catalyst is highly efficient and chemoselective for the reduction of diverse nitro compounds to the corresponding amines.

In summary, the direct pyrolysis of ZIF-67 leads to Co–CoO@N-doped porous carbon nanocomposites. When the optimized catalyst, Co-500-3 h, was applied to a tandem process of NH_3BH_3 dehydrogenation and subsequent hydrogenation of nitro compounds, strikingly, the reduction reaction rate increased exponentially (1100 times higher), compared to that using 1 bar H_2. Moreover, the stable and inexpensive Co-500-3 h exhibits high chemoselectivity and magnetic recyclability in the reduction of a variety of aliphatic and aromatic nitro compounds. In addition to the excellence of the catalyst, the key to the sharp enhancement in the reaction rate is also attributed to the rapid hydrogen generation from NH_3BH_3, which enables high-concentration hydrogen to be distributed throughout the reaction solution, and greatly increases the probability of contact between the hydrogen and nitro compounds, thus boosting the reaction activity. In contrast to the traditional reduction of nitro compounds with high-pressure hydrogen, the current tandem route at room temperature is not only much more efficient but is also much safer, as stored/pressurized hydrogen is not necessary. On the whole, the pyrolysis of MOFs reported here is a facile and versatile approach to afford nanocomposite catalysts for diverse reactions, and the tandem catalysis strategy in the current work might open up an avenue to boost the catalytic efficiency in many other reactions.

This work was supported by the NSFC (21371162, 51301159, 21521001), the 973 program (2014CB931803), NSF of Anhui Province (1408085MB23), the Recruitment Program of Global Youth Experts and the Fundamental Research Funds for the Central Universities (WK2060190026, WK2060190065).

Notes and references

1 (*a*) N. Ono, *The Nitro Group in Organic Synthesis*, Wiley-VCH, New York, 2001; (*b*) R. S. Downing, P. J. Kunkeler and H. van Bekkum, *Catal. Today*, 1997, **37**, 121; (*c*) A. Corma and P. Serna, *Science*, 2006, **313**, 332; (*d*) H.-U. Blaser, H. Steiner and M. Studer, *ChemCatChem*, 2009, **1**, 210.

2 (*a*) S. Nishimura, *Heterogeneous Catalytic Hydrogenation*, John Wiley & Sons, 2001; (*b*) B. Cornils and W. A. Herrmann, *Applied Homogeneous Catalysis with Organometallic Compounds*, Wiley-VCH, Weinheim, Germany, 2nd edn, 2002.

3 (*a*) R. V. Jagadeesh, A.-E. Surkus, H. Junge, M.-M. Pohl, J. Radnik, J. Rabeah, H. Huan, V. Schünemann, A. Brückner and M. Beller, *Science*, 2013, **342**, 1073; (*b*) Z. Wei, J. Wang, S. Mao, D. Su, H. Jin, Y. Wang, F. Xu, H. Li and Y. Wang, *ACS Catal.*, 2015, **5**, 4783; (*c*) R. K. Rai, A. Mahata, S. Mukhopadhyay, S. Gupta, P.-Z. Li, K. T. Nguyen, Y. Zhao, B. Pathak and S. K. Singh, *Inorg. Chem.*, 2014, **53**, 2904.

4 H.-C. Zhou and S. Kitagawa, *Chem. Soc. Rev.*, 2014, **43**, 5415.

5 (*a*) H.-L. Jiang, B. Liu, Y.-Q. Lan, K. Kuratani, T. Akita, H. Shioyama, F. Zong and Q. Xu, *J. Am. Chem. Soc.*, 2011, **133**, 11854; (*b*) T. K. Kim, K. J. Lee, J. Y. Cheon, J. H. Lee, S. H. Joo and H. R. Moon, *J. Am. Chem. Soc.*, 2013, **135**, 8940; (*c*) J.-K. Sun and Q. Xu, *Energy Environ. Sci.*, 2014, **7**, 2071.

6 (*a*) S. Q. Ma, G. A. Goenaga, A. V. Call and D.-J. Liu, *Chem. – Eur. J.*, 2011, **17**, 2063; (*b*) Y.-X. Zhou, Y.-Z. Chen, L. Cao, J. Lu and H.-L. Jiang, *Chem. Commun.*, 2015, **51**, 8292; (*c*) Y.-Z. Chen, C. Wang, Z.-Y. Wu, Y. Xiong, Q. Xu, S.-H. Yu and H.-L. Jiang, *Adv. Mater.*, 2015, **27**, 5010; (*d*) S. Zhao, H. Yin, L. Du, L. He, K. Zhao, L. Chang, G. Yin, H. Zhao, S. Liu and Z. Tang, *ACS Nano*, 2014, **8**, 12660; (*e*) W. Zhong, H. Liu, C. Bai, S. Liao and Y. Li, *ACS Catal.*, 2015, **5**, 1850; (*f*) W. Xia, A. Mahmood, R. Zou and Q. Xu, *Energy Environ. Sci.*, 2015, **8**, 1837.

7 (*a*) P. Chen, Z. Xiong, J. Luo, J. Lin and K. L. Tan, *Nature*, 2002, **420**, 302; (*b*) W. Grochala and P. P. Edwards, *Chem. Rev.*, 2004, **104**, 1283; (*c*) C. W. Hamilton, R. T. Baker, A. Staubitz and I. Manners, *Chem. Soc. Rev.*, 2009, **38**, 279; (*d*) J. Huang, Y. Tan, J. Su, Q. Gu, R. Černý, L. Ouyang, D. Sun, X. Yu and M. Zhu, *Chem. Commun.*, 2015, **51**, 2794; (*e*) L. Ouyang, J. Tang, Y. Zhao, H. Wang, X. Yao, J. Liu, J. Zou and M. Zhu, *Sci. Rep.*, 2015, **5**, 10776; (*f*) L. Z. Ouyang, X. S. Yang, M. Zhu, J. W. Liu, H. W. Dong, D. L. Sun, J. Zou and X. D. Yao, *J. Phys. Chem. C*, 2014, **118**, 7808; (*g*) M. Zhu, H. Wang, L. Z. Ouyang and M. Q. Zeng, *Int. J. Hydrogen Energy*, 2006, **31**, 251.

8 (*a*) M. Chandra and Q. Xu, *J. Power Sources*, 2006, **156**, 190; (*b*) U. B. Demirci and P. Miele, *Energy Environ. Sci.*, 2009, **2**, 627; (*c*) H.-L. Jiang, S. K. Singh, J.-M. Yan, X.-B. Zhang and Q. Xu, *ChemSusChem*, 2010, **3**, 541; (*d*) M. Zahmakıran, Y. Tonbul and S. Özkar, *J. Am. Chem. Soc.*, 2010, **132**, 6541; (*e*) Q. Yao, Z.-H. Lu, Y. Wang, X. Chen and G. Feng, *J. Phys. Chem. C*, 2015, **119**, 14167; (*f*) Z. Zhang, Z.-H. Lu, H. Tan, X. Chen and Q. Yao, *J. Mater. Chem. A*, 2015, **3**, 23520.

9 (*a*) H. Göksu, S. F. Ho, Ö. Metin, K. Korkmaz, A. M. Garcia, M. S. Gültekin and S. Sun, *ACS Catal.*, 2014, **4**, 1777; (*b*) Q.-H. Yang, Y.-Z. Chen, Z. U. Wang, Q. Xu and H.-L. Jiang, *Chem. Commun.*, 2015, **51**, 10419; (*c*) C. E. Hartmann, V. Jurčík, O. Songis and C. S. J. Cazin, *Chem. Commun.*, 2013, **49**, 1005.

10 R. Banerjee, A. Phan, B. Wang, C. Knobler, H. Furukawa, M. O'Keeffe and O. M. Yaghi, *Science*, 2008, **319**, 939.

11 (*a*) M. C. Biesinger, B. P. Payne, A. P. Grosvenor, L. W. M. Lau, A. R. Gerson and R. St. C. Smart, *Appl. Surf. Sci.*, 2011, **257**, 2717; (*b*) J. Zhu, K. Kailasam, A. Fischer and A. Thomas, *ACS Catal.*, 2011, **1**, 342.

12 (*a*) S. B. Kalidindi, M. Indirani and B. R. Jagirdar, *Inorg. Chem.*, 2008, **47**, 7424; (*b*) H.-L. Jiang, T. Akita and Q. Xu, *Chem. Commun.*, 2011, **47**, 10999.

